Improvement of Heart Function After Transplantation of Encapsulated Stem Cells Induced with miR-1/Myocd in Myocardial Infarction Model of Rat

Samaneh Khazaei[1], Masoud Soleimani[2,3], Seyed Hossein Ahmadi Tafti[4], Rouhollah Mehdinavaz Aghdam[5] , and Zohreh Hojati[1]

Abstract

Cardiovascular disease is one of the most common causes of death worldwide. Mesenchymal stem cells (MSCs) are one of the most common sources in cell-based therapies in heart regeneration. There are several methods to differentiate MSCs into cardiac-like cells, such as gene induction. Moreover, using a three-dimensional (3D) culture, such as hydrogels increases efficiency of differentiation. In the current study, mouse adipose-derived MSCs were co-transduced with lentiviruses containing microRNA-1 (*miR-1*) and Myocardin (*Myocd*). Then, expression of cardiac markers, such as NK2 homeobox 5(*Nkx2-5*), GATA binding protein 4 (*Gata4*), and troponin T type 2 (*Tnnt2*) was investigated, at both gene and protein levels in two-dimensional (2D) culture and chitosan/collagen hydrogel (CS/CO) as a 3D culture. Additionally, after induction of myocardial infarction (MI) in rats, a patch containing the encapsulated induced cardiomyocytes (iCM/P) was implanted to MI zone. Subsequently, 30 days after MI induction, echocardiography, immunohistochemistry staining, and histological examination were performed to evaluate cardiac function. The results of quantitative real -time polymerase chain reaction (qRT-PCR) and immunocytochemistry showed that co-induction of *miR-1* and *Myocd* in MSCs followed by 3D culture of transduced cells increased expression of cardiac markers. Besides, results of in vivo study implicated that heart function was improved in MI model of rats in iCM/P-treated group. The results suggested that *miR-1/Myocd* induction combined with encapsulation of transduced cells in CS/CO hydrogel increased efficiency of MSCs differentiation into iCMs and could improve heart function in MI model of rats after implantation.

Keywords

cardiovascular disease, miR-1, 3D culture, encapsulation, differentiation, mesenchymal stem cells, transplantation

Introduction

Cardiovascular disease (CVD) is main reason of death globally[1]. In the recent decades, there have been significant advances in surgical techniques and pharmacological therapies. Nevertheless, CVDs have remained a leading cause of heart failure worldwide[2]. For this reason, it seems necessary

[1] Department of Cell and Molecular Biology, Faculty of Biological Science and Technology, Isfahan University, Isfahan, Iran
[2] Tissue Engineering and Hematology Department, Faculty of Medical Sciences, Tarbiat Modares University, Tehran, Iran
[3] Tissue Engineering and Nanomedicine Research Center, School of Advanced Technologies in Medicine, Shahid Beheshti University of Medical Sciences, Tehran, Iran
[4] Research Center for Advanced Technologies in Cardiovascular Medicine, Tehran heart Center, Tehran University of Medical Sciences, Tehran, Iran
[5] School of Metallurgy & materials Engineering, College of Engineering, University of Tehran, Tehran, Iran

Corresponding Authors:
Zohreh Hojati, University of Isfahan Faculty of Sciences isfahan Isfahan, 1463677833 Iran.
Email: z.hojati@sci.ui.ac.ir

Masoud Soleimani, Tarbiat Modares University Jalal-e-al ahmad Highway Tehran, 14115-111 Iran.
Email: soleim_m@modares.ac.ir

to adopt new methods, such as cardiac regenerative approaches and cell-based therapies[3]. Among cellular sources, mesenchymal stem cells (MSCs) are widely used due to their unique properties including paracrine effects, strong immunomodulation, low immunogenicity[4], and differentiation ability into several cell lines like cardiomyocyte[5]. MSCs are found in various sources, such as bone marrow, placenta, cord blood, and adipose tissue[6]. Among these, adipose-derived MSCs have several advantages such as their accessibility, easy harvesting, low morbidity, and high expansion capacity[7]. Recently, combined strategies, such as genetic modification[8] and using biomaterials[9] have been developed to increase therapeutic efficacy of MSCs.

In several studies, using genetic modification, MSCs have been differentiated into induced cardiomyocyte-like cells (iCMs), for which both different genes and microRNAs (miRNAs) are used[10–12]. The miRNAs bind to the 3′ untranslated region (3′ UTR) of target genes and down-regulate the expression of them[13]. Various studies implicate that miRNAs are involved in cell proliferation, differentiation, and development[14]. Moreover, different miRNAs are involved in cardiogenesis, which are known as cardiac miRNAs, such as *miR-208a/b, miR-499, miR-133a*, and *miR-1*. The *miR-1* and *miR-133* are involved in early stages of cardiogenesis, while *miR-208a/b* and *miR-499* regulate late stages of cardiac development[15]. The *miR-1* is one of miRNAs differentiating MSCs into cardiomyocyte-like cells by induction of NK2 homeobox 5(*Nkx2.5*) and GATA binding protein 4(*Gata4*) (earliest cardiac markers) expression and activating Wnt/β-catenin signaling pathway[16].

In muscle differentiation, serum response factor (SRF) acts as an activator of muscle genes including *miR-1*[17]. However, it has been shown that SRF is a weak activator, requiring a co-activator called as Myocardin (Myocd) to function properly. SRF and Myocd synergistically increase *miR-1* expression by binding to *miR-1* enhancer sequences[18]. In this regard, herein, the effect of simultaneous overexpression of *miR-1* and *Myocd* on differentiation of MSCs into iCMs was investigated.

Despite many advances in genetic modification of MSCs and their differentiation into iCMs, these cells are not sufficiently effective in cell-based therapy because MSC-derived cardiomyocytes in a two-dimensional (2D) cell culture are often immature and have a phenotype similar to that of fetal cardiomyocyte instead of adult cardiomyocyte[19]. Therefore, many studies have investigated various approaches of 3D cell culture, such as using polymer scaffold, decellularized extracellular matrix, and different hydrogels for further differentiation and maturation of MSCs[20–22]. Furthermore, in myocardial infarction (MI) models, most of the cells injected straightly in infarction zone would undergo apoptosis[23]. Therefore, for increasing retention of the injected cells as well as protecting them from apoptosis in the infarction site, appropriate scaffolds can be utilized to improve healing process[23].

Hydrogels as the first water-swollen biomaterials used in tissue engineering can create a 3D structure[24]. Chitosan is one of the widely used materials in hydrogels because of its properties such as biodegradability, biocompatibility, hydrophilicity, non-toxicity, and compressive strength due to its positive charge[25]. In cardiac regeneration, chitosan has been used in various studies as a cell carrier, increasing cell retention and viability, improving heart function by reducing infarct size and neovascularization in MI model[26–28].

One of the strategies in tissue engineering is the use of composite hydrogels. Chitosan-collagen (CS/CO) hydrogel is one of the most widely used composite hydrogels to improve cardiac cell differentiation and regeneration[29]. Collagen is one of the main components of extracellular matrix promoting tensile strength in heart wall. Collagen promotes survival, proliferation, and cell attachment[30]. Nevertheless, it has high biodegradability rate with weak mechanical strength[31]. But due to mechanical stability and positive charge of chitosan, combination of chitosan and collagen improves mechanical strength and reduces degradation rate of collagen[32]. Thus, in the current study, the effect of simultaneous induction of *miR-1* and *Myocd* on differentiation of MSCs into iCMs in 2D and 3D cultures (CS/CO hydrogel) was investigated. In addition, iCMs encapsulated in CS/CO hydrogel were transplanted in MI model of rats and various tests were performed to evaluate improvement of heart function.

Materials and Methods

Fabrication of Composite Hydrogel

Composite hydrogel consisting of chitosan (CS), human collagen type I (CO), and β-glycerophosphate (β-GP), as a cross-linker, was fabricated according to the previous studies [33]. Briefly, CS and CO (Sigma Aldrich, UK) were dissolved in 0.1 N and 0.02 N acetic acid and were stirred for 6 h to make 2.0% w/w and 4 mg/ml of stock solution, respectively. Then, CS and CO solutions were mixed in a ratio of 3:1 and β-GP (7.5%) was added dropwise as a cross-linker on ice bath. Next, the solution was pipetted into a 48-well plate and gel formation was performed by addition of sterile saturated NaHCO3 at 37°C for 15 min. In order to investigate the porous structure, the hydrogel was freeze-dried at -80°C for 48 h. Subsequently, the freeze-dried samples were covered with gold particles and were studied by a scanning electron microscope (SEM) (Hitachi, SU3500) with 15 kV of accelerating voltage.

Physiochemical Properties of CS/CO Hydrogel

Compressive strength of CS and CS/CO hydrogels was measured on a mechanical test machine (Model: INSTRON 5566). All the samples were compressed to 50% of their initial height and compressive strength of each sample was calculated with respect to compressive strain ratio. For testing swelling ratio, the freeze-dried samples were allowed to hydrate in phosphate-buffered saline (PBS) at room temperature (RT). The swollen samples were weighed at 50 minute-intervals, after removal of

excess PBS by gentle blotting. Swelling ratio was calculated as follows: Q = (Ms-Md) / Md; where Q is swelling ratio, Ms is mass at the swollen state, and Md is mass at the dried state. Finally, Fourier-transform infrared (FTIR) spectroscopy was performed for evaluation of chemical structure of CS and CS/CO. FTIR spectrum was documented at the range of 400 - 4000 cm^{-1}, using KBr pellet by FTIR spectrophotometer (FT-IR 8400 S, Shimadzu, Japan).

Isolation and Characterization of MSCs

Isolation and characterization of MSCs was mentioned in supplementary file.

Lentiviral Production and Transduction of MSCs

For lentiviral generation of *miR-1* and *Myocd*, HEK-293 T cell line (Pasteur institute, Iran) was cultured at a concentration of 3×10^6 cells in 10-cm plates. The mmu-mir-1 vector (containing the cytomegalovirus (CMV) and Simian virus 40(SV40) promoters) (Applied Biological Materials, Canada, mm10023), as well as Myocd (abm, 3130606) and pLenti-III-miR-GFP-Blank (abm, m001) as control were separately co-transfected with psPAX2 (containing gag/pol element) and pMD2. G (vesicular stomatitis virus (VSV) element) into HEK-293 T cell line using Lipofectamine 2000 transfection reagent (Invitrogen, USA) according to the manufacturer's protocols. Then, 48 and 72 h after transfection, the supernatant containing lentiviral particles were collected. Collected viruses were concentrated by ultracentrifuge at 40000 g for 2 h at 4°C.

MSCs at passage 3 were used for transduction. The cells were seeded at a concentration of 4×10^5 in 6-cm petri dishes and the next day were transduced in three groups; first a group of cells that were transduced with pLenti-GFP-blank lentiviruses containing green fluorescent protein (GFP) (MSC^{null}), another group of cells that were infected with *miR-1* lentiviruses containing GFP (MSC^{miR-1}), and the third group of cells that were transduced with both of *miR-1* and *Myocd* lentiviruses containing GFP (MSC$^{miR-1/Myocd}$). The fourth group consisting of non-transduced MSCs was considered as a control (MSC). The composition of the medium used during transduction is the same as the composition of the medium during cell culture, that composed high glucose DMEM, FBS10%, penicillin (100U/ml), and streptomycin (100μg/ml). For transduction, a mixture of the concentrated viruses and polybrene (8 μg/mL) was added into the MSCs at a multiplicity of infection (MOI) of 30. Infection efficiency was evaluated 3 days after transduction by examination of GFP expression using a fluorescence microscope (Olympus, Tokyo, Japan). After puromycin selection (2μg/ml), the transduced cells were cultivated in fresh medium containing DMEM (Gibco, USA) supplemented with 10% FBS (Gibco, USA) for 21 days.

Viability Assay of Transduced Cells

For evaluating their viability, transduced cells were pipetted in equal volumes at a concentration of 1×10^4 in 96-well plate and were kept at 37°C for 7, 14, and 21 days. Cell viability rate was determined by 3-(4,5-dimethyl-2-thiazolyl)-2,5-diphenyl-2 H -tetrazolium bromide (MTT; Sigma Aldrich) assay. At given time points, 100 μl/well of MTT was added into the cells, then was kept at 37°C for 4 h, followed by adding 100 μl/well of dimethyl sulfoxide (DMSO). The samples were monitored at 580 nm of wavelength using enzyme-linked immunosorbent assay (ELISA) reader. The non-transduced MSCs were used as a control.

Evaluation of Differentiation of Transduced Cells

Measuring expression levels of miR-1 *and* Myocd, *and target genes in transduced cells by qRT-PCR.* For verifying transduction efficiency, expression levels of *miR-1* and *Myocd* in treated and control groups was evaluated by quantitative real-time polymerase chain reaction (qRT-PCR) technique. Total RNA was extracted from the transduced cells on day 4 using TRIzol reagent (Invitrogen, USA) according to the manufacturer's instructions. Moreover, total RNA was isolated from different groups of transduced cells and MSCs control group on 7, 14, and 21 days after transduction for evaluation of *Tnnt2*, *Nkx2-5* and *Gata4* expression. cDNA was obtained through reverse transcription of total RNA by cDNA synthesis kit (Takara, Korea). Then, qRT-PCR was performed by SYBR Green PCR master mix (Ampliqon) in an Applied Biosystems 7500 real -time PCR system, according to the manufacturer's protocol. Glyceraldehyde 3-phosphate dehydrogenase (*Gapdh*) was used as the house keeping gene for target gene expression and U6 small nuclear RNA (*U6*) was selected as the house keeping gene for miRNA expression. The $2^{-\Delta\Delta Ct}$ approach was used for data analysis. The sequences of primers used for target amplification are listed in Table 1.

Immunocytochemistry (ICC) analysis. Twenty-one day after transduction in the 48-well plate, fixation of MSCs^{miR-1} and MSCs$^{miR-1/Myocd}$ was performed by 4% paraformaldehyde (PFA) for 20 min at RT and permeabilization was performed with 0.2% Triton X-100 (Sigma, USA) for 5 min at RT. Then, cells were incubated overnight with primary antibodies, at 4 °C. cTnT (ab8295, Abcam, MA, UK), NKX2-5 (ab272914) and GATA4 (ab227512) were used as primary antibodies. Subsequently, cells were incubated with fluorescence-labeled secondary antibodies for 1 h at RT. The cells nuclei were stained with 0.1μg/ml of blue-fluorescent 4', 6-Diamidino-2-phenylindole (DAPI) DNA stain (Sigma, USA) at RT for 5 min. Finally, cells were observed by a fluorescence microscope (Olympus, Tokyo, Japan). ICC analysis for MSCs group was mentioned in supplementary file.

Table 1. Sequences of Primers Used in qRT-PCR.

Gene symbol	Primer	Product size (bp)
miR-1	F: GTAGGCACCTGAAATGGAA	85
	R: TTGATGGTGCCTACAGTACAT	
U6	F: CTCGCTTCGGCAGCACA	94
	R: AACGCTTCACGAATTTGCGT	
Myocd	F: CAAGCCAAAGGTGAAGAAGC	177
	R: TAGCTGAATCGGTGTTGCTG	
Gata4	F: TCATCTCACTACGGGCACAG	233
	R: GGGAAGAGGGAAGATTACGC	
Nkx2-5	F: CCTCAACAGCTCCCTGACTC	201
	R: GGGGACAGCTAAGACACCAG	
Tnnt2	F: GGCAGCTGCTGTTCTGAGGGAG	191
	R: TGCCCTGGTCTCCTCGGTCT	
Gapdh	F: CCTGGAGAAACCTGCCAAGTA	148
	R: GGCATCGAAGGTGGAAGAGT	

3D Cell Culture

Cell viability and proliferation assay for encapsulated cells into CS/CO hydrogel was performed and non-transduced MSCs were used because of eliminate transduction interference on viability test results. For this regard, MSCs were encapsulated to CS/CO hydrogel and were homogenized by stirrer for 1 min. After transferring the mixture to the culture plate, it was neutralized using sterile saturated NaHCO3 solution to pH level of 7, and then it was incubated at 37°C for 15 min. Finally, cell culture medium was added to the encapsulated cells.

Viability and proliferation assays in CS/CO hydrogel. For evaluating their viability, MSCs were pipetted in equal volumes with a density of 1×10^5 in 96-well plate and were kept at 37°C for 1, 3,7, and 14 days. Cell viability rate was examined by MTT assay, as previously described. Cell free hydrogel and 2D culture of MSCs were used as control. Moreover, for showing cell proliferation potential in the hydrogel, the cells were labeled with 1,1'-dioctadecyl-3,3,3',3' –tetramethylindocarbocyanine perchlorate (DiI) (Thermofisher), a red cell membrane dye, according to manufacturer's instructions. Finally, on days 1, 3, and 7, fluorescence microscopy was performed.

SEM analysis. Twenty-one days after transduction, the MSCs embedded in hydrogel was prepared for SEM analysis. The medium was aspirated, and glutaraldehyde (2.5%) was added to the cells and they were kept for 1 h at 4°C and after washing with PBS, dehydration was performed by ascending series of ethanol and SEM was performed as previously described [34].

Encapsulation of Transduced Cells in CS/CO Hydrogel and Evaluation of their Differentiation into iCMs

3 days after transduction, MSCs[miR-1/Myocd] were trypsinized and encapsulated in CS/CO hydrogel. Then, like the 2D culture, qRT-PCR and ICC assay for differentiation assessment of encapsulated transduced cells were performed. Total RNA was obtained from the cells on 7, 14, and 21 days after infection. Subsequently, after cDNA synthesis, qRT-PCR was performed for evaluation of *Tnnt2*, *Nkx2-5,* and *Gata4* expression. MSCs[miR-1/Myocd] in 2D culture was used as a control group. Moreover, ICC assay was implemented on MSCs[miR-1/Myocd] for cTnT, NKX2-5 and GATA4 markers.

In vivo Studies

Induction of myocardial infarction (MI) in rats and patch transplantation. In the current study, 20 male Sprague Dawley (SD) rats (6–8 weeks old, and 180–250 g) were used. All the animal experiments were conducted according to the guidelines approved by Care and Use of Laboratory Animals and the Ethics Committee of the Tarbiat Modares University, Iran (IR.MODARES.REC.1398.125). The rats were anesthetized by intramuscular injection of 50 ml/kg of ketamine hydrochloride and 5 mg/kg of xylazine. Next, the thoracotomy was performed, the pericardium was opened and a 5-0 silk suture was narrowed close the left anterior descending (LAD) coronary artery. After 10 min, color of the area under the suture was changed and patches were transplanted on MI zone. The transplanted patches (P), comprising of CS/CO hydrogel placed on Polydimethylsiloxane (PDMS) were used in three groups; P (cell-free patch), MSC/P, and iCM/P. In MSC/P and iCM/P groups, MSCs and iCMs were encapsulated in CS/CO hydrogel and then were placed on PDMS. For tracking the transplanted cells in rat heart tissue, DiI staining was used to label cells before transplantation according to manufacturer's structure. In MI group, the LAD was sutured but no patches were transplanted on MI zone. Finally, rats were sacrificed by an intravenous injection of sodium thiopental (100 ml/kg) and the hearts were harvested for qRT-PCR, SEM, and histological analyses.

Echocardiography. Echocardiographic images of the hearts from 20 rats were obtained using a GE Vivid 7 echocardiography machine before MI, 3 days after MI (baseline), and 30 days after MI from different groups. For measuring left ventricular (LV) function, fractional shortening (FS), ejection fraction (EF), End-systolic volume (ESV), and End-diastolic volume (EDV) were assessed by echocardiography. The percentage of fractional shortening (FS) was calculated as follows: FS (%) $=$[(LVEDd$-$LVESd)/LVEDd] $\times$ 100 where LVEDd is LV end-diastolic dimension and LVESd is LV end-systolic dimension. All the measurements were performed based on averaged three sequential cycles of cardiac and were assessed by two independent operators who were blinded to treat and control groups of the animals.

RNA isolation and qRT-PCR analysis. Total RNA isolation, cDNA synthesis, and qRT-PCR were performed for *Tnnt2*, *Nkx2-5*, and *Gata4* genes for intervention and control groups, as previously described. MI group was used as negative control.
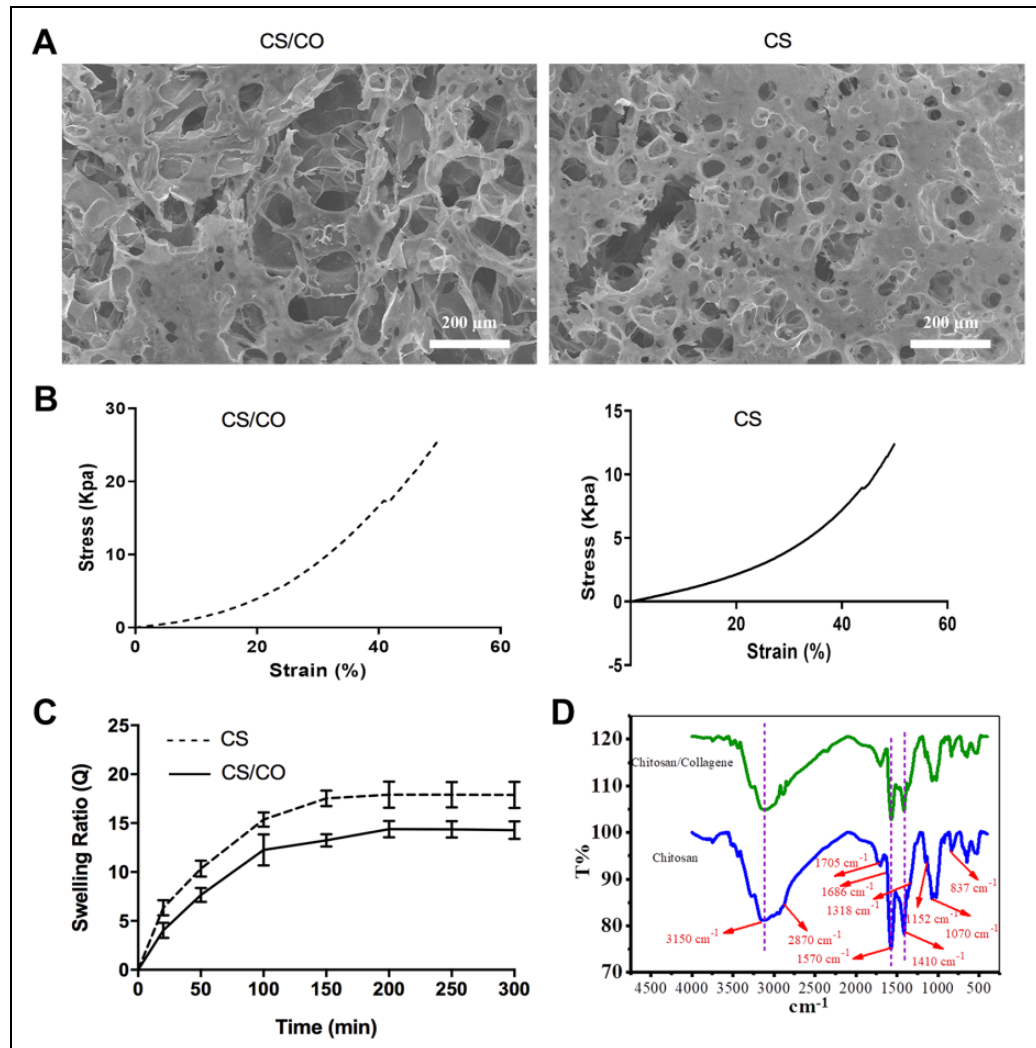
Figure 1. Fabrication and characterization of CS/CO hydrogel. (A) Results of SEM analysis of CS/CO and pure CS hydrogels showed a porous structure. **(B)** Stress-strain curve of CS/CO hydrogel and pure CS showed that CS/CO hydrogel had significantly higher compressive strength than CS. **$P < 0.01$. **(C)** Swelling ratio was significantly lower in CS/CO hydrogel than CS because pure CS is more hydrophilic than CS/CO hydrogel. *$P < 0.05$. **(D)** FTIR spectra of CS and CS/CO hydrogel showed a successful cross-link between CS and CO. CS: Chitosan, CS/CO: Chitosan/collagen, FTIR: Fourier-transform infrared.

Histological analysis and immunohistochemistry (IHC). Samples were prepared for histological analysis according to previous study[35]. Briefly, samples underwent 10% formalin fixation for 24 h and were embedded into paraffin wax. Paraffin-embedded tissues were cut at a thickness of 3μm and were prepared for histological assay. For the routine histological assessment was performed on tissue sections by Hematoxylin and Eosin (H & E) staining[36]. Moreover, IHC analysis was performed according to previous protocols[37] and paraffin-embedded sections were immunostained with cTnT, NKX2-5, and GATA4 antibodies. The images were observed by inverted fluorescence microscope (Olympus, Japan).

Statistical analysis

All data were represented as mean $\pm$ standard deviation (SD) of at least three experiments. The differences between test and control groups were analyzed with the unpaired t-test, one-way or two-way ANOVA using GraphPad Prism v9.0 (USA). *P*-values < 0.05 were regarded to be statistically significant.

Results

Morphology and characterization of the CS/CO hydrogel

SEM analysis was performed for determining morphological structure of CS and CS/CO hydrogels. The composite hydrogel exhibited a structure with CO fibrils dispersed within CS matrix. Moreover, interconnecting pores and creasing patterns were formed inside the hydrogels (Fig. 1A). CS and CS/CO hydrogel showed porous structure with 51.57% and 56.68% porosity, 17–89 μm and 21–109 μm pore size,

respectively. This means that the pore size in both hydrogels allows the exchange of nutrients and biological molecules between cells. Stress-strain curve showed that pure CS and CS/CO hydrogels indicated a gradually enhancement in stiffness. Moreover, the CS/CO hydrogel showed a significant increase (**$P < 0.01$) in compression strength in comparison with the pure CS hydrogel because CO-containing hydrogels are stiffer than pure CS due to higher density (Fig. 1B). As shown in Fig. 1C, the swelling ratio in CS/CO hydrogel was significantly lower than pure CS hydrogel (*$P < 0.05$), because of higher hydrophilicity of CS compared to CO. FTIR spectrum of CS recorded absorption at 3150 cm^{-1} and 2870 cm^{-1}, which are attributed to groups of OH– and CH3–, respectively. In addition, the absorptions observed at 1570 cm^{-1} and 1410 cm^{-1} are related to stretching vibration of N-H group and vibration of OH– group (primary alcohol), respectively. The bond observed at 1318 cm^{-1} and 1070 cm^{-1} corresponds to tensile vibrations of C-O-N and C-O. Additionally, the adsorption intensities observed in 1152 cm^{-1} and 837 cm^{-1} are attributed to glucoside bonds, respectively. The peak observed at 1686 cm^{-1} indicates tensile vibration of C=O and the band seen at 1705 cm^{-1} is related to free acetic acid. FTIR spectrum of the CS / CO hydrogel included all CS or CO adsorption peaks separately. No extra peaks were observed. It should be noted that the interaction between CO and CS occurs through formation of hydrogen bonds. When the amount of CO in the hydrogel is low, intensity of Amide I peak is decreased, whereas intensity corresponding to Amide II is increased. Amide I peak at 1623 cm^{-1} for pure CO was almost not found in the hydrogel sample, but it can be seen in the case of Amide II (the corresponding peak at 1560 cm^{-1}) with a slight change at 1554 cm^{-1} in the hydrogel, proving well the proper interaction between CO and CS. In addition, triple helix continuity in CO can be evaluated at 1235 cm^{-1} and 1450 cm^{-1} peaks. Intensity ratio of these two peaks in pure CO was equal to 1; however, it was increased to 1.06 through addition of CS in the hydrogel, confirming the proper interaction between CO and CS in the hydrogel. On the other hand, this implies that structural properties of CO have been well preserved (Fig. 1D).

Up-Regulation of miR-1 and Myocd Expression in Transduced Cells

Transduction efficiency was performed by fluorescent microscopy and flow cytometry assessment, which about 80% of cells were transduced (Fig. 2A). Expression levels of *miR-1* and *Myocd* were determined on day 4 after transduction in intervention and control groups using qRT-PCR assay. The results indicated that expression of *miR-1* in MSC^{miR-1} and MSC$^{miR-1/Myocd}$ groups was increased by 68- and 88-folds, respectively, compared to MSCs control group. Moreover, Myocd expression was up-regulated by 43- and 57-folds in MSC^{Myocd} and MSC$^{miR-1/Myocd}$ groups, respectively, compared to MSCs control group (Fig. 2B). Expectedly, when MSCs were transduced with empty

lentiviruses, *miR-1* and *Myocd* expression showed no significant changes in comparison with MSCs group. Viability of the transduced cells in intervention groups evaluated by MTT assay was lower than control groups (Fig. 2C).

Differentiation of Transduced Cells into iCM

Seven days after transduction, morphological changes were observed in different groups of transduced cells. On day 7, morphology of MSC^{miR-1} and MSC$^{miR-1/Myocd}$ groups was found to be short spindle- or star-shaped (Fig. 3A). As expected, morphology of control groups (MSC and MSC^{null}) did not change (Data were not shown). Twenty-one days after transduction, further differentiation and maturation was observed. The cells became polygonal or spindle-shaped and were connected to adjacent cells (Fig. 3A).

As shown in Fig. 3B, mRNA expression of the genes involved in cardiogenesis, such as *Nkx2-5* and *Gata4* (key transcription factors), *Tnnt2* (cardiac specific marker) was analyzed by qRT-PCR on days 7, 14, and 21 post-transduction. The results indicated that *Nkx2-5* and *Gata4* genes were expressed at maximum levels 7 days after transduction and then, their expression was gradually decreased, while the maximum level of *Tnnt2* expression was observed on day 14 in MSC^{miR-1} and MSC$^{miR-1/Myocd}$ groups. The results also indicated that expression levels of target genes were significantly higher in the MSC$^{miR-1/Myocd}$ group than the MSC^{miR-1}. For ICC analysis, MSC^{miR-1} and MSC$^{miR-1/Myocd}$ were immunostained with cTnT, NKX2.5, and GATA4 antibodies on day 21 after transduction. The images indicated that the markers in the MSC$^{miR-1/Myocd}$ group were more upregulated than the MSC^{miR-1} group (Fig. 3C). The results confirmed that *Myocd* gene had a synergistic effect on *miR-1* expression resulting in increased expression of cardiac markers. Images of MSCs ICC analysis was mentioned in supplementary file (Fig. S2).

Viability and Proliferation Analyses of Cells in CS/CO Hydrogel

For viability and proliferation analysis of composite hydrogel, MSCs were encapsulated in CS/CO hydrogel. Dil staining of the encapsulated cells in the CS/CO hydrogel showed that the cells were proliferated over time (Fig. 4A). In addition, quantified results regarding assessment of proliferation showed that the number of DiI-positive encapsulated cells were significantly increased on days 3 and 7 compared to day 1 (*$P < 0.05$, **$P < 0.01$, respectively) (Fig. 4B). In addition, viability and proliferation assays were performed for 1, 3, 7, and 14 days after 3D culture. The MTT assay results showed percentage of surviving cells grown in the CS/CO hydrogel. Fig. 4C illustrates that the cells had the ability to survive in the hydrogel at different time points. Cell free hydrogel and 2D culture of MSCs were used as control. Besides, 21 days after encapsulation, MSCs were prepared for SEM analysis. As shown in Fig. 4D, the cells
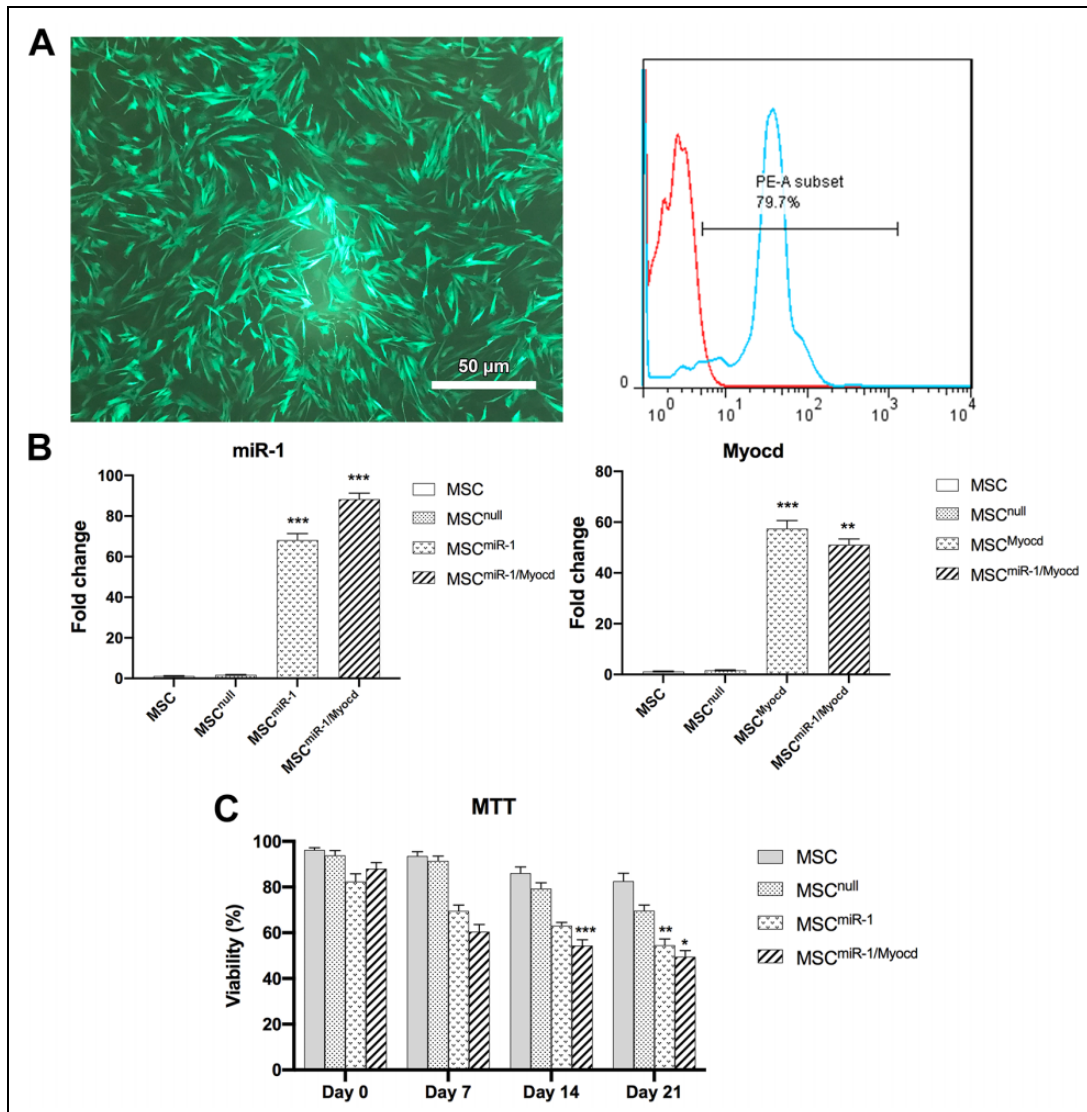
Figure 2. Transduction efficiency of MSCs with lentiviruses containing miR-1 and Myocd. (A) Transduced cells were observed by fluorescence microscopy regarding expression of GFP reporter. Moreover, percentage of transduced cells was measured by flow cytometry. About 80% of MSCs were transduced compared to the control cells. **(B)** Expression of *miR-1* and *Myocd* in different groups was evaluated by qRT-PCR. **$P < 0.01$, ***$P < 0.001$; data were expressed as mean $\pm$ SD, $n = 3$. **(C)** Cell viability of transduced cells was studied by MTT analysis. In intervention groups, cell viability was significantly reduced on days 14 and 21. *$P < 0.05$, **$P < 0.01$, ***$P < 0.001$. GFP: Green fluorescent protein.

were well attached and encapsulated inside the hydrogel with round morphologies.

Differentiation of Encapsulated Transduced Cells in CS/CO Hydrogel

3 days after transduction, transduced cells (MSC$^{miR-1/Myocd}$) were trypsinized and cultured in CS/CO hydrogel. Subsequently, qRT-PCR and ICC analysis were performed to evaluate the differentiation of encapsulated cells. As in the 2D culture, mRNA gene expression of *Tnnt2*, *Nkx2-5* and *Gata4,* were measured 7, 14, and 21 days after transduction. According to Fig. 5A, expression level of target genes in encapsulated transduced cells were significantly increased

compared to the transduced cells in 2D cell culture (*$P < 0.05$). Additionally, ICC images showed that the expression of cardiac markers in 3D culture were upregulated in comparison with 2D culture (Fig. 5B). Taken together, these results implicated that encapsulation of transduced cells into CS/CO hydrogel promotes the differentiation of MSCs into iCMs, due to increased cell-cell and cell-environment interactions.

Effect of iCM/P on Cardiac Function

After MI induction (Fig. 6A), transplantation of patch was performed in different groups (Fig. 6B). Echocardiograph analysis was performed 30 days after patch transplantation
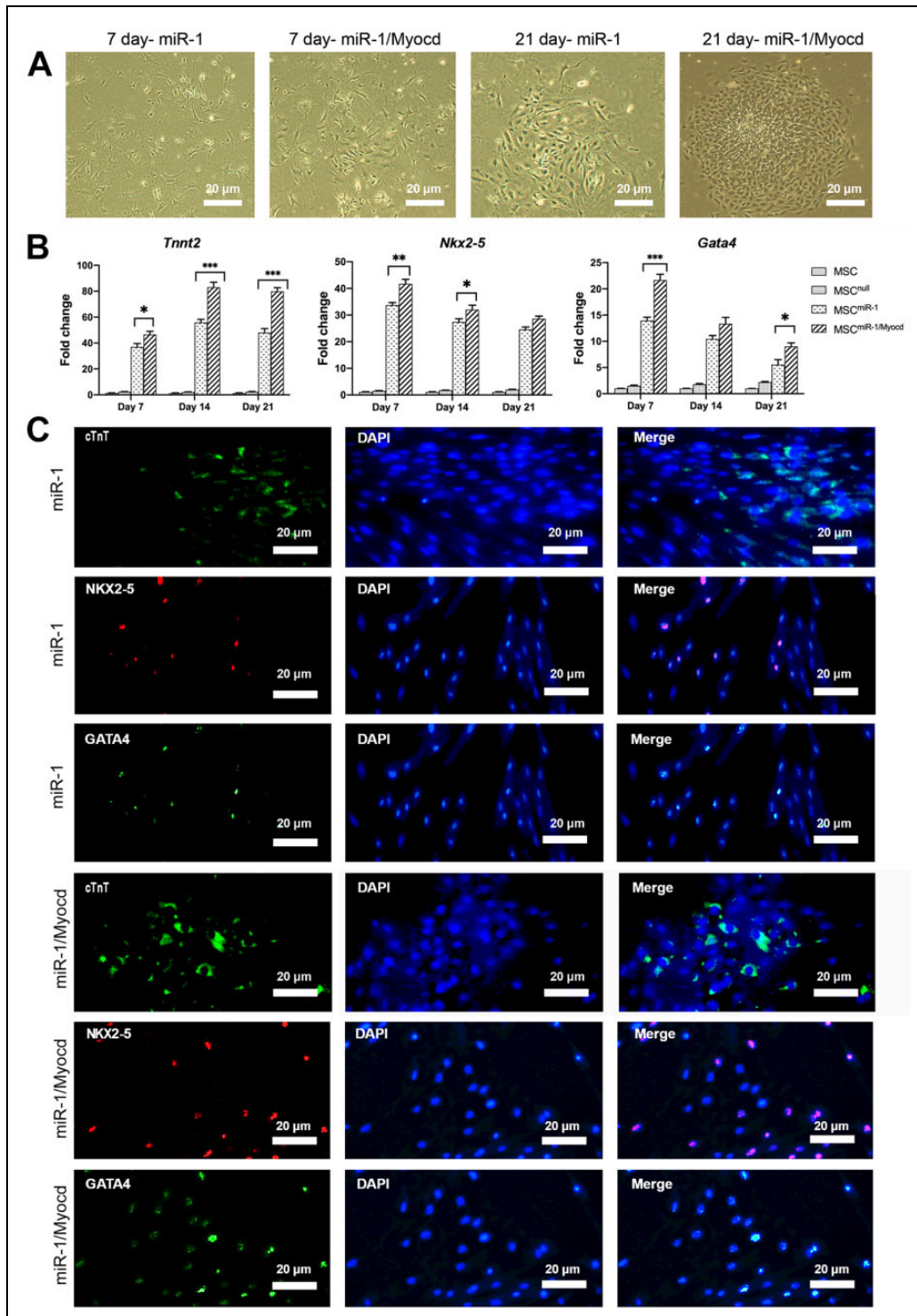
Figure 3. Differentiation of transduced cells into iCMs. (A) Seven days after transduction, morphology of MSC^{miR-1} and MSC$^{miR-1/Myocd}$ groups became spindle-shaped or star-shaped. Twenty-one days after transduction, the cells became more differentiated and matured and short spindle-shaped or polygonal cells were observed, similar to cardiomyocytes. **(B)** qRT-PCR analysis was performed for cardiac specific markers of *Tnnt2*, *Nkx2-5*, and *Gata4*. Expression of markers was compared in MSC^{miR-1} and MSC$^{miR-1/Myocd}$ groups with MSC^{null} as a negative control. The results showed that expression of *Tnnt2*, *Nkx2-5*, and *Gata4* was increased significantly in MSC$^{miR-1/Myocd}$ group in comparison with other groups, on days 7, 14, and 21 after transduction. *$P < 0.05$, **$P < 0.01$, ***$P < 0.001$; Transcript value was shown as mean $\pm$ SD. **(C)** ICC analysis detected cTnT, Nkx2-5, and GATA4 markers in MSC^{miR-1} and MSC$^{miR-1/Myocd}$ groups on day 21. Nucleus staining was conducted by DAPI stain. An Olympus fluorescence microscope was used to record images.
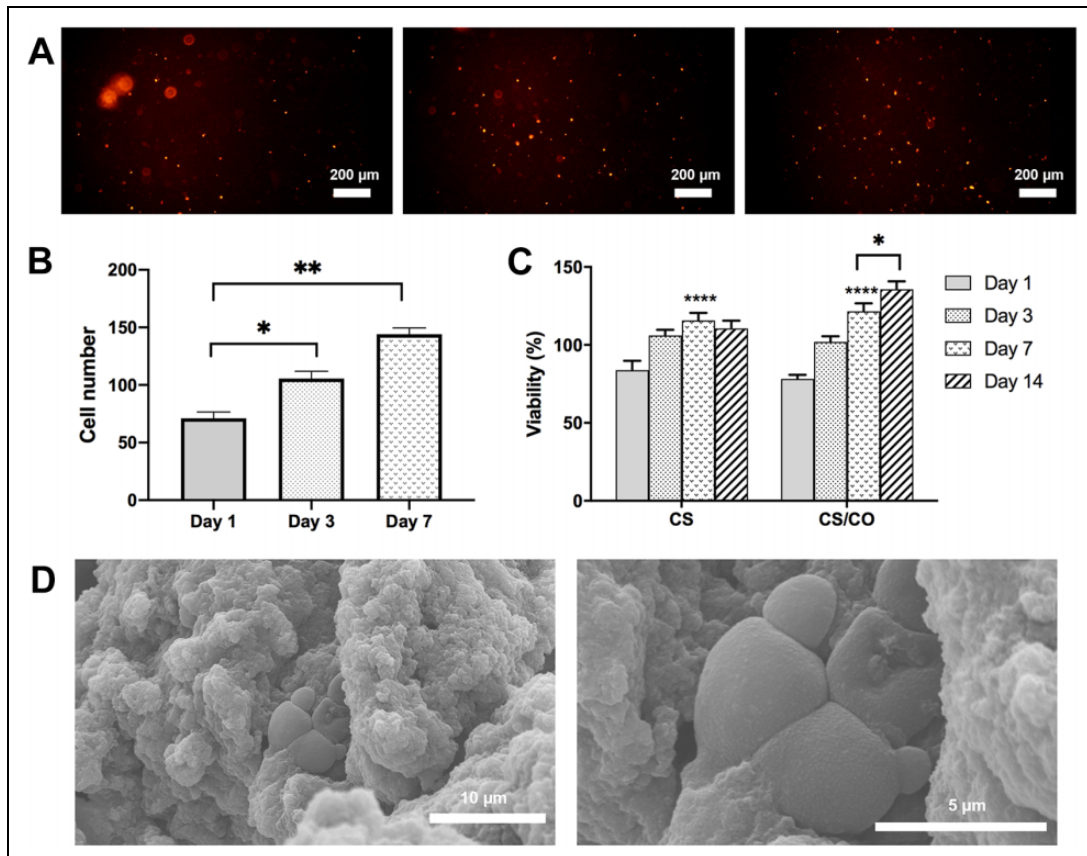
Figure 4. 3D culture of MSCs into the CS/CO hydrogel and viability assay. (A) Dil staining of the encapsulated cells in the CS/CO hydrogel implicated that the cells were proliferated over time. **(B)** The number of the stained cells was increased significantly on day 7 compared to day 1 after cultivation in the CS/CO hydrogel **P < 0.01. **(C)** Results of MTT assay implicated that cell viability percentage was increased significantly on 3, 7, and 14 days after encapsulation in the CS/CO hydrogel. *P < 0.05, ****P < 0.0001. **(D)** SEM image of the encapsulated transduced cells into the CS/CO hydrogel with two magnifications. 3D culture: Three dimensional culture, CS/CO: Chitosan/collagen.

in different groups (Fig. 6C). The increased EF and FS in both iCM/P and MSC/P groups indicated functional recovery after cell/patch transplantation in comparison with MI control group. Additionally, the increase in EF and FS was significantly higher in the iCM/P group compared to MSC/P group by *P < 0.05 and **P < 0.01, respectively. A significant decrease in EDV and ESV was found 30 days after MI compared to 3 days after MI in the iCM/P group (Fig. 6D), meaning that 30 days after MI induction in the intervention group, volume of blood remaining in the heart ventricle was reduced after ejection, similar to normal heart.

Effect of iCM/P on Cardiac gene Expression in MI Zone

The expression levels of *Tnnt2*, *Nkx2-5*, and *Gata4* was significantly increased in iCM/P group with mean fold changes of 10.4, 7.2, and 5, respectively compared to MI control group. Moreover, expression of the genes was significantly increased in iCM/P group much more than MSC/P group (**P < 0.01) (Fig. 7A). Besides, in Patch group, expression of target genes did not show a significant difference in comparison with MI group.

Histological and IHC Staining in MI Zones

For histological examination, H&E staining was performed for MI zone of patch transplantation-treated and MI groups. As shown in Fig. 7B, myocytes in iCM/P and MSC/P groups were arranged regularly and vascular structures and red blood cells were detectable. In contrast, no regularly and vascular structures were detected in MI zone of MI group. On day 30 post-transplantation, the patch-treated groups showed the grafted cells with DiI labeling in MI zone. In heart sections with DiI labeling in iCM/P and MSC/P groups, co-localization of DiI labeling and cTnT, NKX2.5, and GATA4 markers was observed. Expression of markers in Patch and MI groups was observed only in border of MI zones (Fig. 7C).

Discussion

The miRNAs are considered as regulators in bioprocesses, such as differentiation, proliferation, and development and they have important roles in cardiogenesis[38]. Among cardiac-specific miRNAs, *miR-1* is involved in early stage
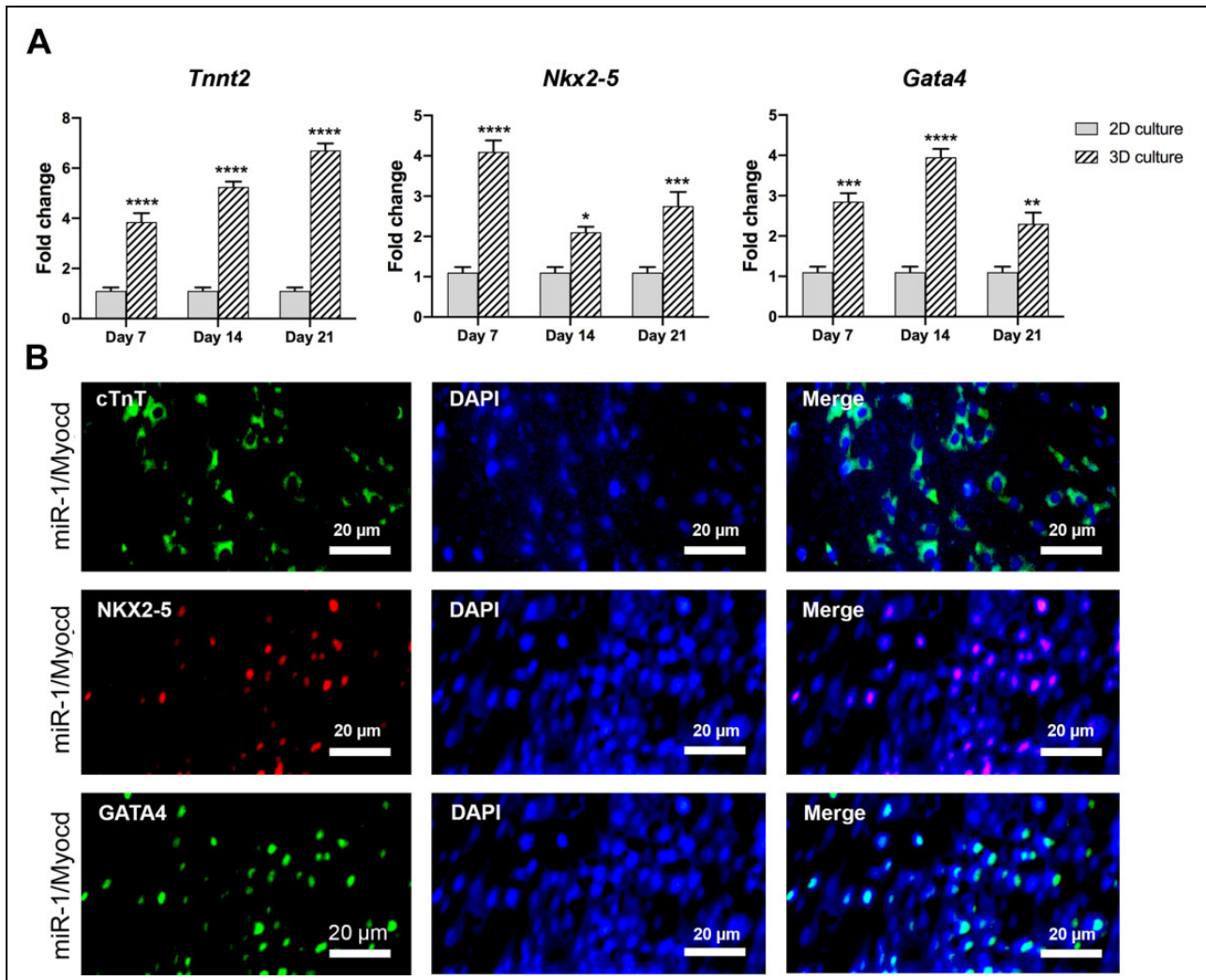
Figure 5. Differentiation of transduced cells into iCM after encapsulation in the CS/CO hydrogel. Three days after co-transduction of MSCs with *miR-1* and *Myocd* lentiviruses, the infected cells were trypsinized and embedded in the CS/CO hydrogel. **(A)** Expression of *Tnnt2*, *Nkx2-5*, and *Gata4*, and was evaluated by qRT-PCR in 2D and 3D cell cultures (CS/CO hydrogel). Expression of markers was increased significantly in the 3D cell culture in comparison with the 2D cell culture. $*P < 0.05$, $**P < 0.01$, $***P < 0.001$, $****P < 0.0001$; Transcript value was shown as mean $\pm$ SD. **(B)** Immunofluorescence staining of transduced cells 21 days after transduction showed that expression of the markers was enhanced in 3D culture. iCMs: Induced cardiomyocytes, CS/CO: Chitosan/collagen, 3D culture: Three dimensional culture.

of cardiomyocyte development by targeting different signaling pathways including Wnt/β-catenin pathway. Various studies have shown that miR-1 activates Wnt/β-catenin signaling pathway by downregulation of genes that are inhibitor of Wnt pathway. Activation of the Wnt/β-catenin pathway has been found to enhance expression of genes, such as *wnt11*, β-*catenin*, *c-Jun N-terminal kinase (JNK)*, and *ternary complex factor(TCF)*, which in turn enhanced expression of cardiac- specific genes including *Nkx2-5*, *Gata4*, and *Tnnt2*[16]. Also, level of cardiac miRNAs, in particular miR-1 has been indicated to be increased in differentiation of MSCs into iCMs. Therefore, *miR-1* overexpression causes further differentiation of MSCs into iCMs via targeting Wnt pathway and regulation of target genes expression[39]. Myocyte enhancer factor-2 (Mef2), SRF, and Myocd are *miR-1*

transcriptional activators, binding to its enhancer sequences. Myocd is a co-activator for SRF because it is a weak activator. Thus, Myocd is an important factor for *miR-1* expression in early stages of heart development[17]. Moreover, in various studies, the effect of Myocd on cardiac cell differentiation and enhancement of cardiac genes expression has been investigated[40,41]. Zhang et al. studied transdifferentiation of fibroblasts into iCMs by transduction of miR-1 alone or in combination with five cardiac transcription factors including GATA4, T-box transcription factor 5 (TBX5), Mef2, MYOCD, and NKX2-5 (GTMMN). TNNT2^{+} cells were significantly enhanced when *miR-1* was used in combination with GTMMN[42]. In the current study, co-transduction effect of *miR-1* and *Myocd* was evaluated on efficacy of MSCs differentiation into iCMs. Consistent with
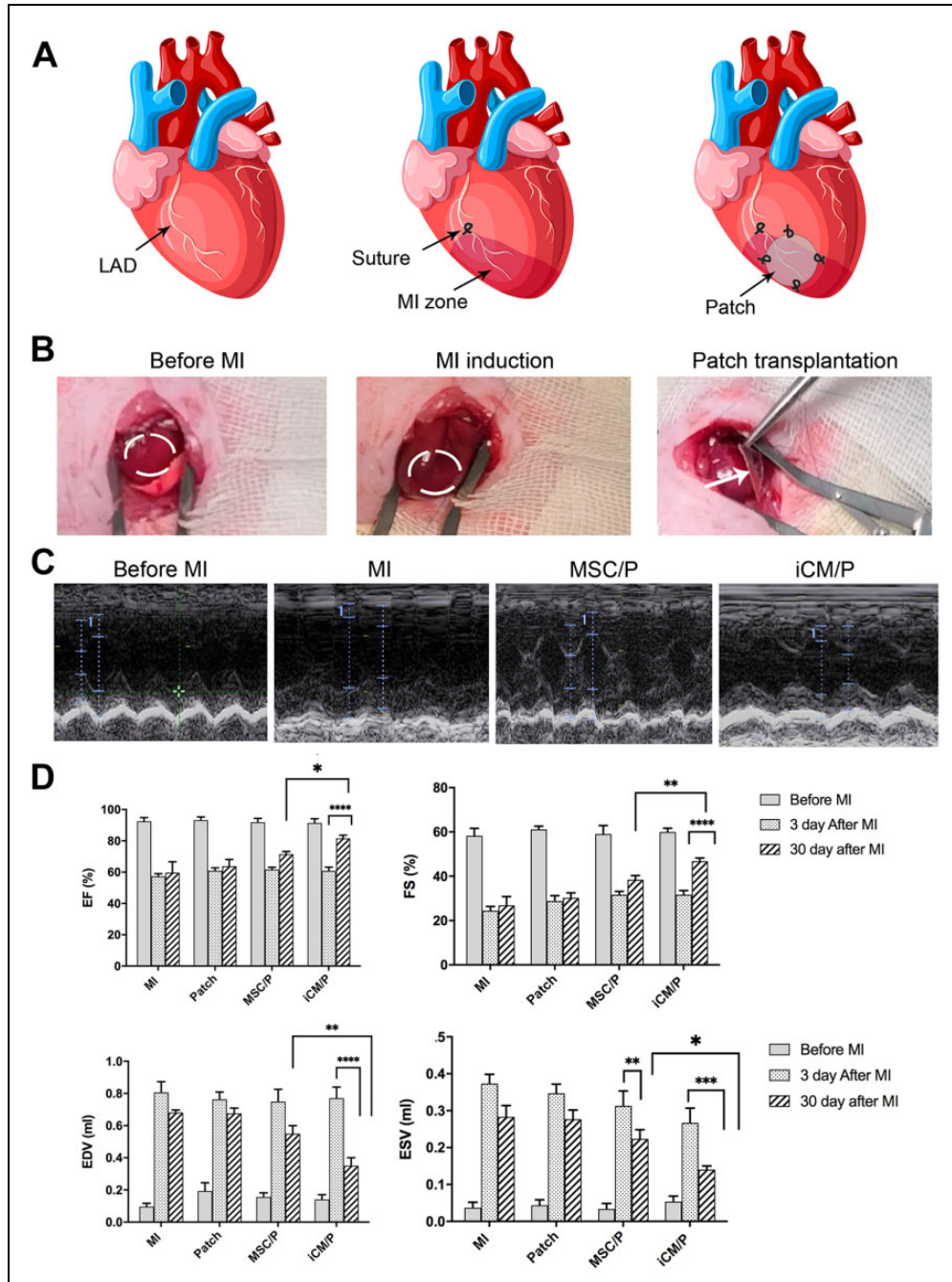
Figure 6. Evaluation of heart function after patch transplantation. (A) Schematic representation of the heart before and after MI induction and patch transplantation. **(B)** MI induction was performed by tightening the silk suture around the LAD. After changing color of the area, patch containing CS/CO, placed on PDMS, was transplanted on the MI zone. **(C)** Representative M-mode echocardiogram of the MI, P, MSC/P, and iCM/P groups is shown. D) FS, EF, ESV, and EDV values of different groups were quantified. FS and EF values were increased significantly in MSC/P and iCM/P groups versus MI group. Moreover, ESV and EDV values were significantly reduced in MSC/P and iCM/P groups compared to MI group. In addition, FS and EF values were enhanced significantly in iCM/P group versus MSC/P group. *$P < 0.05$, **$P < 0.01$, ***$P < 0.001$, ****$P < 0.0001$. MI: Myocardial infarction, LAD: Left anterior descending, PDMS: Polydimethylsiloxane, FS: Fractional shortening, EF: Ejection fraction, ESV: End-systolic volume, EDV: End-diastolic volume, iCMs: Induced cardiomyocytes.

the previous studies[40,42], our results showed that expression of cardiac markers including *Tnnt2*, *Nkx2-5*, and *Gata4* at gene and protein levels was higher in MSCs transduced with a combination of *miR-1* and *Myocd* than MSCs transduced with *miR-1* alone.

Most studies on cells function have been performed in 2D microenvironment, but recently 3D culture has been developed because of its advantages over 2D culture. In 3D cell culture, different cells interact with each other and with extracellular matrix. Whereas, in 2D cell culture, cells
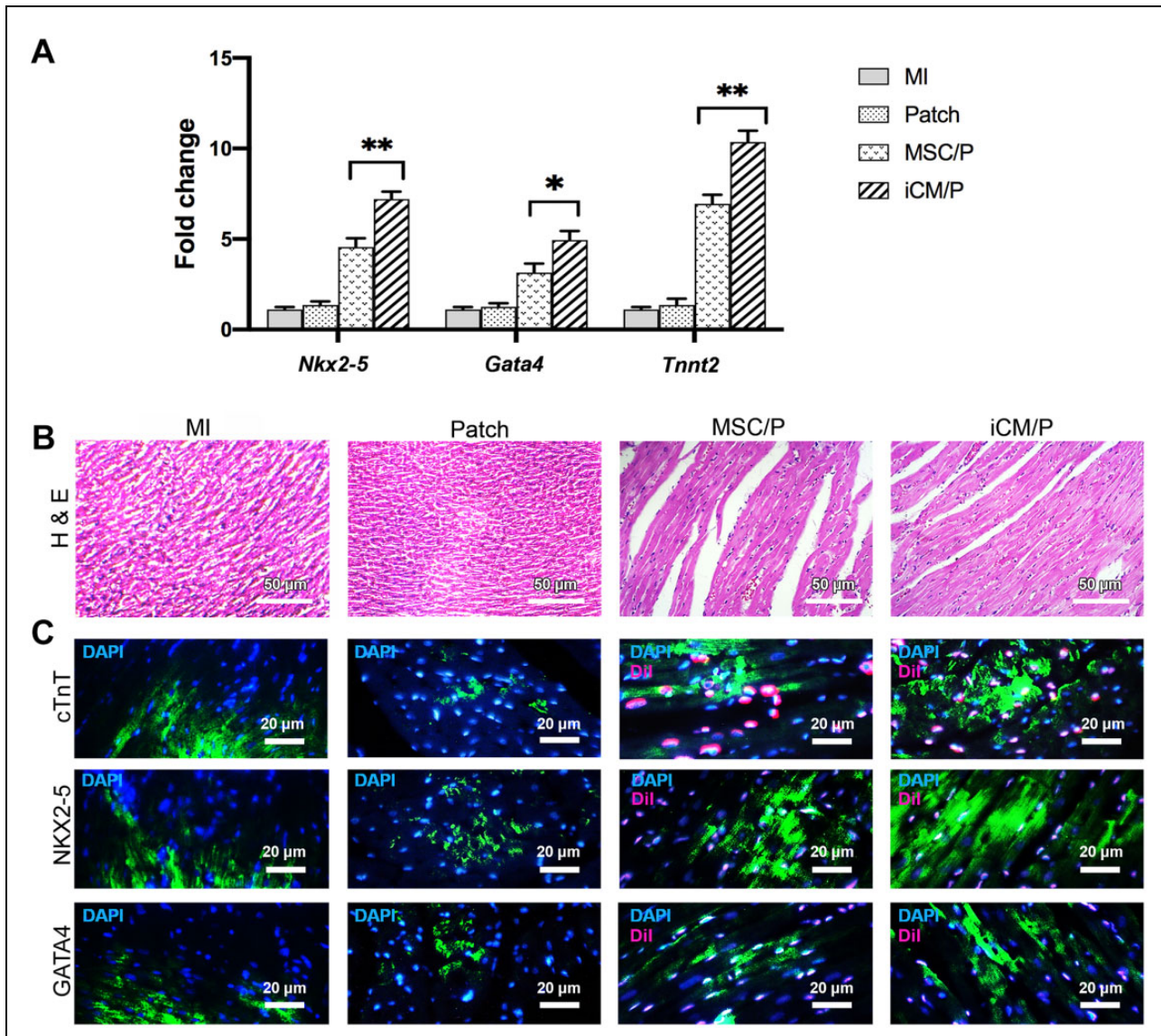
Figure 7. qRT PCR, histological studies and immunohistochemical staining of heart tissues after patch implantation.
(A) qRT-PCR assessment of MI zone tissue in the intervention and control groups. **(B)** Histological analysis showed that myocytes in iCM/P group had regularly structure and red blood cells were observed, while in MI group, inflammatory cells infiltrated in MI zone and large area of fibrosis was detectable. **C)** Thirty days after MI induction, IHC staining was performed for NKX2-5, GATA4, and cTnT markers of MI zone tissue. The images showed that the immunostained cells in the iCM/P group were more than the other groups. Encapsulated cells of iCM/P and MSC/P groups were labeled with Dil stain for tracking in rats heart tissues.

interact only with their surrounding cells[43,44]. In addition, mechanical forces between cell-cell and cell-environment in 3D culture provide a set of signals, regulating different functions of cells, such as proliferation, differentiation, and migration[45]. Moreover, structure and organization of cells in 3D culture change compared to a 2D culture, influencing function and cell signaling[46]. Therefore, it can be concluded that cell behaviors in 3D culture are different from 2D culture.

3D culture promotes an environment for better signaling between cells and their neighboring, and causes more realistic physiological, biomechanical, and biochemical

properties, and less substrate stiffness than 2D environment, collectively increasing differentiation capability of MSCs into different cell lines. A combination of these conditions alters gene expression of MSCs and thus, activates different signaling pathways ultimately improving efficacy of MSCs differentiation[47]. Pineda et al., investigated myocardial differentiation of embedded mouse embryonic stem cells (M-ESCs) in collagen type I gels (GELs)[48]. They indicated that expression of *Gata4*, *FMS-like tyrosine kinase 1(Flt1)*, and *endothelin type B receptor (Endbr)* was upregulated in GELs compared to 2D culture. As a result, 3D culture is a supportive environment for cardiovascular differentiation.

Hydrogels are more common than other biomaterials due to their properties, such as similarity to natural extracellular matrices (ECM), biocompatibility, encapsulation of cells, integrating with host cells, and enhancement of cell proliferation, survival, and differentiation[49].

CS as a biocompatible polysaccharide is frequently used in tissue engineering due to its antioxidant activity, lack of immunogenicity, and bioactive properties[26]. Studies have shown that CS as a scaffold in combination with MSCs can improve heart function in MI models of rats[27,28]. There are several mechanisms for improving function of ischemic heart and reduction of infarct size for example, (1) CS, as a carrier of MSCs increases their survival and engraftment, which is related to antioxidant activity of CS and eliminating of reactive oxygen species (ROS), diminishing cell adhesion, and eventually improving MI environment[50]. (2) CS is involved in formation of neovasculature. In addition, MSCs in combination with CS play a synergistic role in ischemic myocardial angiogenesis because they have paracrine effect and release angiogenic factors like vascular endothelial growth factor (VEGF), basic fibroblast growth factor (b-FGF), and hepatocyte growth factor (HGF)[51]. (3) CS increases differentiation of MSCs into cardiac-like cells due to collagen synthesis[28]. CO is one of the main components of ECM playing an important role in process of cardiac maturation and differentiation of MSCs[30]. Therefore, heart function is improved by replacing cardiac differentiated cells in MI zone.

CO facilitates cell adhesion by integrin receptors, activating signaling pathways, which in turn regulate cell survival, proliferation, and differentiation[30]. Therefore, in combination with CS, efficiency of differentiation of MSCs into cardiac-like cells is improved. Moreover, due to similarity of CO to the pericardium and native ECM, and enhancement of tensile strength, composite hydrogel of CS and CO improves heart function in a MI model of rat[33]. The prepared integrated porous CS/CO hydrogel network provided a microenvironment for cell proliferation and differentiation by permeability of nutrients and biological molecules and development of signaling pathway among embedded cells in hydrogel[33]. Moreover, the presence of CO in the hydrogel increases compaction. As a result, CS/CO hydrogel is more compact and stiffer than pure CS[33]. Additionally, results of viability test and Dil staining showed that the composite CS/CO hydrogel promoted growth and proliferation of the encapsulated cells and had no cytotoxicity effect. In the current study, first mouse MSCs were co-transduced with *miR-1* and *Myocd* lentiviruses, and after 3 days, the transduced cells were encapsulated in CS/CO hydrogel to improve efficiency of differentiation and maturation. In the encapsulated cells, expression of cardiac markers of *Tnnt2*, *Nkx2-5*, and *Gata4*, and, at levels of gene and protein was significantly upregulated in comparison with the transduced cells in 2D culture.

Previous studies have shown that transplantation of MSCs in MI zone does not effectively improve heart function due to high apoptosis rate of the transplanted cells in the infarct environment and low efficiency of their differentiating into cardiomyocytes and endothelial cells[48,52]. Therefore, recently, using different hydrogels has been considered for injection or transplantation of MSCs in the MI zone[53,54]. In the present report, for in vivo studies, after co-transduction of MSCs with miR-1 and Myocd lentiviruses, iCMs were encapsulated into CS/CO hydrogel followed by placed on PDMS for making patch. PDMS is a biocompatible and biodegradable substrate that has been shown in several studies to use as a substrate to promote the self-renewal and differentiation of stem cells into cardiomyocyte[58]. PDMS have also been used in several studies as a suitable substrate for cultivation[59] and implantation[60].

After MI induction, patches were implanted to the MI zone in different groups including iCM/P, MSC/P, and cell-free/P groups. Echocardiography of rat heart tissue was performed for assessing heart function. The results confirmed that EF and FS were increased in iCM/P and MSC/P groups, indicating an improvement in the impaired heart function after transplantation of the encapsulated cells[55]. Moreover, cardiac markers, at the level of gene and protein, in iCM/P group significantly increased in comparison with control group.

As mentioned in previous studies[56,57], MSCs transplantation in MI zone can partially improve heart function due to induction of angiogenesis, paracrine effects, and stimulating differentiation of the implanted MSCs into cardiomyocyte. In the iCM/P group, not all MSCs are differentiated into iCMs, and this group includes a heterogeneous population of differentiated iCMs and undifferentiated MSCs. Therefore, in the iCM/P group, both iCMs and MSCs are effective in improving heart function after MI induction. As a result, in the MSC/P group, a relative improvement in heart function is observed.

Conclusion

Our results revealed that co-induction of miR-1 and Myocd followed by culture in CS/CO hydrogel led to greater differentiation and maturation of MSCs. Additionally, heart function was improved after transplantation of encapsulated iCMs in MI model of rat. Therefore, our findings indicated importance of 3D culture in stem cell differentiation. So, in the future studies, progress in cardiac regeneration based on cell therapy can be achieved by improving differentiation conditions of MSCs and subsequently, obtaining mature cardiac cells.

Declaration of Conflicting Interests

The author(s) declared no potential conflicts of interest with respect to the research, authorship, and/or publication of this article.

Ethics approval

Ethical approval to report this case was obtained from the Ethics Committee of the Tarbiat Modares University, Iran (IR.MODARES.REC.1398.125).

Statement of human and animal rights

All procedures in this study were conducted in accordance with the Ethics Committee of the Tarbiat Modares University, Iran (IR.MODARES.REC.1398.125) approved protocols.

Statement of informed consent

There are no human subjects in this article and informed consent is not applicable.

ORCID iDs

Rouhollah Mehdinavaz Aghdam [ID] https://orcid.org/0000-0003-2325-5121
Zohreh Hojati [ID] https://orcid.org/0000-0003-4831-0123

Supplemental Material

Supplemental material for this article is available online.

References:

1. Zhao Y, Londono P, Cao Y, Sharpe EJ, Proenza C, O'Rourke R, Jones KL, Jeong MY, Walker LA, Buttrick PM, McKinsey TA, et al. High-efficiency reprogramming of fibroblasts into cardiomyocytes requires suppression of pro-fibrotic signalling. Nat Commun. 2015;6:1–15.

2. Muiesan ML, Paini A, Rosei CA, Bertacchini F, Stassaldi D, Salvetti M. Current pharmacological therapies in heart failure patients. High Blood Press Cardiovasc Prev. 2017;24(2): 107–114.

3. Hénon P. Key success factors for regenerative medicine in acquired heart diseases. Stem Cell Rev Rep. 2020;16(3): 441–458.

4. Karantalis V, Hare JM. Use of mesenchymal stem cells for therapy of cardiac disease. Circ Res. 2015;116(8):1413–1430.

5. Ohnishi S, Ohgushi H, Kitamura S, Nagaya N. Mesenchymal stem cells for the treatment of heart failure. Int J Hematol. 2007;86(1):17–21.

6. Musialek P, Mazurek A, Jarocha D, Tekieli L, Szot W, Kostkiewicz M, Banys RP, Urbanczyk M, Kadzielski A, Trystula M, Kijowski J, et al. Myocardial regeneration strategy using Wharton's jelly mesenchymal stem cells as an off-the-shelf 'unlimited' therapeutic agent: results from the Acute Myocardial Infarction First-in-Man study. Postepy Kardiol Interwencyjne. 2015;11(2):100.

7. Perin EC, Sanz-Ruiz R, Sánchez PL, Lasso J, Pérez-Cano R, Alonso-Farto JC, Pérez-David E, Fernández-Santos ME, Serruys PW, Duckers HJ, Kastrup J, et al. Adipose-derived regenerative cells in patients with ischemic cardiomyopathy: the PRECISE trial. Am Heart J. 2014;168(1):88–95. e82.

8. Park JS, Suryaprakash S, Lao YH, Leong KW. Engineering mesenchymal stem cells for regenerative medicine and drug delivery. Methods. 2015;84:3–16.

9. Martino S, D'Angelo F, Armentano I, Kenny JM, Orlacchio A. Stem cell-biomaterial interactions for regenerative medicine. Biotechnol Adv. 2012;30(1):338–351.

10. McGinley L, McMahon J, Strappe P, Barry F, Murphy M, O'Toole D, O'Brien T. Lentiviral vector mediated modification of mesenchymal stem cells & enhanced survival in an in vitro model of ischaemia. Stem Cell Res Ther. 2011;2(2):1–18.

11. Satija NK, Singh VK, Verma YK, Gupta P, Sharma S, Afrin F, Sharma M, Sharma P, Tripathi RP, Gurudutta GU. Mesenchymal stem cell-based therapy: a new paradigm in regenerative medicine. J Cell Mol Med. 2009;13(11–12):4385–4402.

12. Neshati V, Mollazadeh S, Bazzaz BS, De Vries AA, Mojarrad M, Naderi-Meshkin H, Neshati Z, Mirahmadi M, Kerachian MA. MicroRNA-499a-5p promotes differentiation of human bone marrow-derived mesenchymal stem cells to cardiomyocytes. Appl Biochem Biotechnol. 2018;186(1):245–255.

13. Treiber T, Treiber N, Meister G. Regulation of microRNA biogenesis and its crosstalk with other cellular pathways. Nat Rev Mol Cell Biol. 2019;20(1):5–20.

14. Torrini C, Cubero RJ, Dirkx E, Braga L, Ali H, Prosdocimo G, Gutierrez MI, Collesi C, Licastro D, Zentilin L, Mano M. Common regulatory pathways mediate activity of microRNAs inducing cardiomyocyte proliferation. Cell Rep. 2019;27(9); 2759–2771. e2755.

15. Piubelli C, Meraviglia V, Pompilio G, D'Alessandra Y, Colombo GI, Rossini A. microRNAs and cardiac cell fate. Cells. 2014;3(3):802–823.

16. Shen X, Pan B, Zhou H, Liu L, Lv T, Zhu J, Huang X, Tian J. Differentiation of mesenchymal stem cells into cardiomyocytes is regulated by miRNA-1-2 via WNT signaling pathway. J Biomed Sci. 2017;24(1):1–8.

17. Zhao Y, Samal E, Srivastava D. Serum response factor regulates a muscle-specific microRNA that targets Hand2 during cardiogenesis. Nature. 2005;436(7048):214–220.

18. Wang DZ, Chang PS, Wang Z, Sutherland L, Richardson JA, Small E, Krieg PA, Olson EN. Activation of cardiac gene expression by myocardin, a transcriptional cofactor for serum response factor. Cell. 2001;105(7):851–862.

19. Fong AH, Romero-López M, Heylman CM, Keating M, Tran D, Sobrino A, Tran AQ, Pham HH, Fimbres C, Gershon PD, Botvinick EL. Three-dimensional adult cardiac extracellular matrix promotes maturation of human induced pluripotent stem cell-derived cardiomyocytes. Tissue Eng Part A. 2016; 22(15–16):1016–1025.

20. Caspi O, Lesman A, Basevitch Y, Gepstein A, Arbel G, Habib IH, Gepstein L, Levenberg S. Tissue engineering of vascularized cardiac muscle from human embryonic stem cells. Circ Res. 2007;100(2);263–272.

21. Bejleri D, Davis ME. Decellularized extracellular matrix materials for cardiac repair and regeneration. Adv Healthc Mater. 2019;8(5):1801217.

22. Saludas L, Pascual-Gil S, Prósper F, Garbayo E, Blanco-Prieto M. Hydrogel based approaches for cardiac tissue engineering. Int J Pharm. 2017;523(2):454–475.

23. Anderl JN, Robey TE, Stayton PS, Murry CE. Retention and biodistribution of microspheres injected into ischemic myocardium. J Biomed Mater Res A. 2009;88(3):704–710.

24. Spicer CD. Hydrogel scaffolds for tissue engineering: the importance of polymer choice. Polymer Chemistry. 2020; 11(3):184–219.

25. Fukuda J, Khademhosseini A, Yeo Y, Yang X, Yeh J, Eng G, Blumling J, Wang CF, Kohane DS, Langer R. Micromolding of photocrosslinkable chitosan hydrogel for spheroid microarray and co-cultures. Biomaterials. 2006;27(30):5259–5267.

26. Cui Z, Ni NC, Wu J, Du GQ, He S, Yau TM, Weisel RD, Sung HW, Li RK. Polypyrrole-chitosan conductive biomaterial synchronizes cardiomyocyte contraction and improves myocardial electrical impulse propagation. Theranostics. 2018;8(10):2752.

27. Chen J, Zhan Y, Wang Y, Han D, Tao B, Luo Z, Ma S, Wang Q, Li X, Fan L, Li C. Chitosan/silk fibroin modified nanofibrous patches with mesenchymal stem cells prevent heart remodeling post-myocardial infarction in rats. Acta Biomater. 2018;80:154–168.

28. Wang H, Shi J, Wang Y, Yin Y, Wang L, Liu J, Liu Z, Duan C, Zhu P, Wang C. Promotion of cardiac differentiation of brown adipose derived stem cells by chitosan hydrogel for repair after myocardial infarction. Biomaterials. 2014;35(13):3986–3998.

29. Wang H, Shi J, Wang Y, Yin Y, Wang L, Liu J, Liu Z, Duan C, Zhu P, Wang C. Synthesis and characterization of injectable hydrogels with varying collagen–chitosan–thymosin β4 composition for myocardial infarction therapy. J Funct Biomater. 2018;9(2):33.

30. Orgel JP, Persikov AV, Antipova O. Variation in the helical structure of native collagen. PLoS One. 2014;9(2):e89519.

31. Orgel JP, Persikov AV, Antipova O. Collagen–chitosan polymer as a scaffold for the proliferation of human adipose tissue-derived stem cells. J Mater Sci Mater Med. 2009;20(3): 799–808.

32. Deng C, Zhang P, Vulesevic B, Kuraitis D, Li F, Yang AF, Griffith M, Ruel M, Suuronen EJ. A collagen–chitosan hydrogel for endothelial differentiation and angiogenesis. Tissue Eng Part A. 2010;16(10):3099–3109.

33. Wang L, Stegemann JP. Thermogelling chitosan and collagen composite hydrogels initiated with β-glycerophosphate for bone tissue engineering. Biomaterials. 2010;31(14): 3976–3985.

34. Koroleva A, Deiwick A, Nguyen A, Schlie-Wolter S, Narayan R, Timashev P, Popov V, Bagratashvili V, Chichkov B. Osteogenic differentiation of human mesenchymal stem cells in 3-D Zr-Si organic-inorganic scaffolds produced by two-photon polymerization technique. PloS One. 2015;10(2);e0118164.

35. Baudouy D, Michiels JF, Vukolic A, Wagner KD, Wagner N. Echocardiographic and histological examination of cardiac morphology in the mouse. J Vis Exp. 2017;26(128):55843.

36. Valentin J, Frobert A, Ajalbert G, Cook S, Giraud MN. Histological quantification of chronic myocardial infarct in rats. J Vis Exp. 2016;11(118):54914.

37. Yang G, Tian J, Feng C, Zhao LL, Liu Z, Zhu J. Trichostatin a promotes cardiomyocyte differentiation of rat mesenchymal stem cells after 5-azacytidine induction or during coculture with neonatal cardiomyocytes via a mechanism independent of histone deacetylase inhibition. Cell Transplant. 2012; 21(5):985–996.

38. Synnergren J, Améen C, Lindahl A, Olsson B, Sartipy P. Expression of microRNAs and their target mRNAs in human stem cell-derived cardiomyocyte clusters and in heart tissue. Physiol Genomics. 2011;43(10):581–594.

39. Zhao XL, Yang B, Ma LN, Dong YH. MicroRNA-1 effectively induces differentiation of myocardial cells from mouse bone marrow mesenchymal stem cells. Artif Cells Nanomed Biotechnol. 2016;44(7):1665–1670.

40. Nam YJ, Song K, Luo X, Daniel E, Lambeth K, West K, Hill JA, DiMaio JM, Baker LA, Bassel-Duby R, Olson EN, et al. Reprogramming of human fibroblasts toward a cardiac fate. Proc Natl Acad Sci U S A. 2013;110(14):5588–5593.

41. Christoforou N, Chellappan M, Adler AF, Kirkton RD, Wu T, Addis RC, Bursac N, Leong KW. Transcription factors MYOCD, SRF, Mesp1 and SMARCD3 enhance the cardio-inducing effect of GATA4, TBX5, and MEF2C during direct cellular reprogramming. PloS one. 2013;8(5):e63577.

42. Christoforou N, Chakraborty S, Kirkton RD, Adler AF, Addis RC, Leong KW. Core transcription factors, microRNAs, and small molecules drive transdifferentiation of human fibroblasts towards the cardiac cell lineage. Sci Rep. 2017;7:1–15.

43. Zhang D, Shadrin IY, Lam J, Xian HQ, Snodgrass HR, Bursac N. Tissue-engineered cardiac patch for advanced functional maturation of human ESC-derived cardiomyocytes. Biomaterials. 2013;34(23):5813–5820.

44. Ronaldson-Bouchard K, Ma SP, Yeager K, Chen T, Song L, Sirabella D, Morikawa K, Teles D, Yazawa M, Vunjak-Novakovic G. Advanced maturation of human cardiac tissue grown from pluripotent stem cells. Nature. 2018;556(7700):239–243.

45. Shadrin IY, Allen BW, Qian Y, Jackman CP, Carlson AL, Juhas ME, Bursac N. Cardiopatch platform enables maturation and scale-up of human pluripotent stem cell-derived engineered heart tissues. Nat Commun. 2017;8(1):1–15.

46. Chaicharoenaudomrung N, Kunhorm P, Noisa P. Three-dimensional cell culture systems as an in vitro platform for cancer and stem cell modeling. World J Stem Cells. 2019; 11(12):1065.

47. Sokolowska P, Zukowski K, Lasocka I, Szulc-Dabrowska L, Jastrzebska E. Human mesenchymal stem cell (hMSC) differentiation towards cardiac cells using a new microbioanalytical method. Analyst. 2020;145(8):3017–3028.

48. Pineda ET, Nerem RM, Ahsan T. Differentiation patterns of embryonic stem cells in two-versus three-dimensional culture. Cells Tissues Organs. 2013;197(5):399–410.

49. Domenech M, Polo-Corrales L, Ramirez-Vick JE, Freytes DO. Tissue engineering strategies for myocardial regeneration: acellular versus cellular scaffolds? Tissue Eng Part B Rev. 2016;22(6):438–458.

50. Liu Z, Wang H, Wang Y, Lin Q, Yao A, Cao F, Li D, Zhou J, Duan C, Du Z, Wang Y. The influence of chitosan hydrogel on

stem cell engraftment, survival and homing in the ischemic myocardial microenvironment. Biomaterials. 2012;33(11): 3093–3106.

51. Yamada Y, Yokoyama SI, Wang XD, Fukuda N, Takakura N. Cardiac stem cells in brown adipose tissue express CD133 and induce bone marrow nonhematopoietic cells to differentiate into cardiomyocytes. Stem Cells. 2007;25(5):1326–1333.

52. Yeh YC, Lee WY, Yu CL, Hwang SM, Chung MF, Hsu LW, Chang Y, Lin WW, Tsai MS, Wei HJ, Sung HW, et al. Cardiac repair with injectable cell sheet fragments of human amniotic fluid stem cells in an immune-suppressed rat model. Biomaterials. 2010;31(25):6444–6453.

53. Fujimoto KL, Ma Z, Nelson DM, Hashizume R, Guan J, Tobita K, Wagner WR. Synthesis, characterization and therapeutic efficacy of a biodegradable, thermoresponsive hydrogel designed for application in chronic infarcted myocardium. Biomaterials. 2009;30(26):4357–4368.

54. Ruvinov E, Leor J, Cohen S. The promotion of myocardial repair by the sequential delivery of IGF-1 and HGF from an injectable alginate biomaterial in a model of acute myocardial infarction. Biomaterials. 2011;32(2):565–578.

55. Chi NH, Yang MC, Chung TW, Chen JY, Chou NK, Wang SS. Cardiac repair achieved by bone marrow mesenchymal stem cells/silk fibroin/hyaluronic acid patches in a rat of myocardial infarction model. Biomaterials. 2012;33(22): 5541–5551.

56. Tao H, Han Z, Han ZC, Li Z. S-nitrosoglutathione reductase (GSNOR) enhances vasculogenesis by mesenchymal stem cells. Proceed Nat Academy Sci. 2013;110(8):2834–2839.

57. Gao XR, Xu HJ, Wang LF, Liu CB, Yu F. Mesenchymal stem cell transplantation carried in SVVYGLR modified self-assembling peptide promoted cardiac repair and angiogenesis after myocardial infarction. Biochem Biophys Res Commun. 2017;491(1):112–118.

58. Fu J., Chuah Y., Liu J., Tan S., Wang D. Respective effects of gelatin-coated polydimethylsiloxane (PDMS) substrates on self-renewal and cardiac differentiation of induced pluripotent stem cells (iPSCs). ACS Biomater Sci Eng. 2018;4(12): 4321–4330.

59. Oyunbaatar NE, Lee DH, Patil SJ, Kim ES, Lee DW. Biomechanical characterization of cardiomyocyte using PDMS pillar with microgrooves. Sensors. 2016;16(8):1258.

60. Jackman CP, Ganapathi AM, Asfour H, Qian Y, Allen BW, Li Y, Bursac N. Engineered cardiac tissue patch maintains structural and electrical properties after epicardial implantation. Biomaterials. 2018;159:48–58.